Journal of the American Heart Association

ORIGINAL RESEARCH

Spatial Correlates of Dementia and Disability After Intracerebral Hemorrhage

Yutong Chen, MB, BChir; Cyprien A. Rivier, MD, MSc; Samantha A. Mora, BSc; Victor Torres Lopez, MSc; Sam Payabvash, MD; Kevin Sheth, MD; Andreas Harloff, MD; Guido J. Falcone, MD, ScD; Jonathan Rosand, MD, MSc; Ernst Mayerhofer, MD† Christopher D. Anderson, MD, MMSc†

BACKGROUND: Dementia and disability are highly prevalent after spontaneous intracerebral hemorrhage (ICH). Previous studies categorizing ICH by large anatomic boundaries have demonstrated that lobar ICH is associated with dementia, while ICH in the basal ganglia is associated with disability. This study aims to refine our understanding of the association between ICH location and post-ICH dementia and disability at a voxel level, which could improve the prognostic accuracy of these outcomes and provide mechanistic insights into post-ICH functional outcomes.

METHODS AND RESULTS: In this cohort study, we segmented the ICH lesions from the noncontrast computed tomography scans from 882 patients from the MGH-ICH (Massachusetts General Hospital ICH Study) as the discovery data set and from 146 patients from the Yale-ICH cohort as the validation data set. Using electronic health records and follow-up telephone interviews, incident dementia (*International Classification of Diseases*, *Ninth Revision* [*ICD-9*] codes of dementia or modified telephone interview for cognitive status <20) and disability (modified Rankin Scale score >2) were identified. The median follow-up times of the MGH-ICH and Yale-ICH cohorts were 2.9 (interquartile range, 1.0–5.8) years and 1.0 (interquartile range, 0.6–1.0) years, respectively. Two techniques of lesion symptom mapping were applied on the ICH lesions: sparse canonical correlation analysis for neuroimaging and voxel-based lesion symptom mappings. Dementia conversion after ICH was associated with ICH in the left temporo-occipital region (mean hazard ratio [HR], 3.62 [95% CI, 2.71–4.63]) and left superior longitudinal fasciculus (mean HR, 2.91 [95% CI, 2.40–3.52]). Development of disability after ICH was linked to the right cerebral peduncle (mean HR, 3.10 [95% CI, 2.44–3.94]), right pallidum (mean HR, 2.96 [95% CI, 1.99–4.25]), and right posterior limb of the internal capsule (mean HR, 2.54 [95% CI, 1.88–3.96]).

CONCLUSIONS: Specific distribution of ICH lesions is linked to development of dementia and disability after ICH. These insights have the potential to enhance clinical prognostic models for patients with ICH, facilitating more precise predictions of outcomes based on hemorrhage location.

Key Words: dementia ■ disability ■ intracerebral hemorrhage ■ voxel-based lesion symptom mapping

Intracerebral hemorrhage (ICH) is associated with high prevalence of post-ICH cognitive impairment[1] and disability.[2] Between 35% and 55% of survivors of ICH developed cognitive impairment,[3] while functional impairment occurred in 61% to 88% cases.[4] Identifying the patients who will develop dementia and disability after ICH is important for planning rehabilitation and counseling for prognosis.

Recent studies have uncovered risk factors for post-ICH dementia and disability. These factors include age, hematoma volume, level of education, and preexisting small-vessel diseases[5,6] for post-ICH dementia;

Correspondence to: Christopher D. Anderson, MD, MMSc, Department of Neurology, Brigham and Women's Hospital, Boston, MA. Email: cdanderson@mgb.org

†E. Mayerhofer and C. D. Anderson contributed equally.

This manuscript was sent to Adriana B. Conforto, MD, PhD, Associate Editor, for review by expert referees, editorial decision, and final disposition.

Supplemental Material is available at https://www.ahajournals.org/doi/suppl/10.1161/JAHA.124.037930

For Sources of Funding and Disclosures, see page 12.

JAHA is available at: www.ahajournals.org/journal/jaha

RESEARCH PERSPECTIVE

What Is New?

- A novel lesion symptom mapping technique, sparse canonical correlation analysis for neuroimaging, was applied alongside voxel-based lesion symptom mappings to decipher the association between intracerebral hemorrhage (ICH) location and post-ICH dementia and disability at a voxel level.
- Dementia conversion after ICH was associated with hematoma in the left temporo-occipital region and left superior longitudinal fasciculus.
- Development of post-ICH disability was associated with lesions in the right basal ganglia and right cerebral peduncle and right posterior limb of the internal capsule.

What Question Should Be Addressed Next?

- Are early- and late-onset post-ICH dementia associated with different spatial distributions of hematomas?
- Can cerebral amyloid angiopathy explain the association between ICH distribution and dementia conversion?

Nonstandard Abbreviations and Acronyms

CAA	cerebral amyloid angiopathy
ICH	intracerebral hemorrhage
LSM	lesion symptom mapping
MGH	Massachusetts General Hospital
MGH-ICH	Massachusetts General Hospital ICH Study
MNI	Montreal Neurological Institute
mRS	modified Rankin scale
PLIC	posterior limb of the internal capsule
SCCAN	sparse canonical correlation analysis for neuroimaging
VLSM	voxel-based lesion-symptom mapping

and age, hematoma volume, intraventricular hemorrhage, and alcohol consumption for disability.[7,8] ICH location significantly influences both outcomes.[5–7,9,10] Lobar ICH is more highly associated with post-ICH dementia.[5] This association may be attributed to the disruption of cortical structures by lobar ICH and its potential connection with underlying cerebral amyloid angiopathy (CAA), which is a risk factor for post-ICH dementia.[6] In post-ICH disability, the thalamus and the internal capsule are strongly implicated[7,11] due to the disruption of the pyramidal tracts in the internal capsule.[12] Traditionally, research has classified ICH by broad anatomic regions, but analyzing ICH outcomes at a voxel level could provide a more detailed understanding of the spatial correlates of post-ICH dementia and disability. This voxel-level analysis could drive the development of more personalized prognostic tools for ICH survivors based on lesion distribution in specific regions.

Lesion symptom mapping (LSM) allows investigation of the spatial correlates of post-ICH dementia and disability at a voxel level. Two key LSM approaches are voxel-based lesion-symptom mapping (VLSM) and sparse canonical correlation analysis for neuroimaging (SCCAN). VLSM applies a statistical test between a clinical outcome and the presence of a lesion in a voxel and repeats this analysis for every voxel.[13,14] VLSM allows for adjustment for confounding variables but suffers from low statistical power.[14] This limitation was addressed by SCCAN, which constructs a single multivariate model to account for the presence of lesions in every voxel simultaneously. The limitations of SCCAN include its inability to adjust for confounding variables and to be applicable in studying longitudinal outcomes. Therefore, we would use both VLSM and SCCAN to complement their respective weaknesses to identify the brain regions associated with post-ICH dementia and disability. We hypothesize that understanding these associations is crucial for developing accurate ICH prognostic tools and for gaining insights into the mechanisms of post-ICH dementia and disability.

METHODS

Data Availability

The source code is published at https://github.com/Yutong441/ICHmap. The data sets presented in this article are not available because of ethical and privacy restrictions.

Cohort Characteristics

This study employed the MGH-ICH (Massachusetts General Hospital ICH Study) cohort, a single-center, longitudinal cohort consisting of patients with primary ICH at Massachusetts General Hospital (MGH) between 1994 and 2019. Patients were prospectively recruited. During their admission, imaging and medical records were gathered. After discharge, phone interviews were conducted at 3, 6, 9, and 12 months, followed by interviews every 6 months thereafter. The median follow-up time is 2.9 (interquartile range [IQR], 1.0–5.8) years. The study was approved by the

Mass General Brigham Institutional Review Board (IRB2006P000570).

To validate the results in the MGH-ICH cohort, we used the Yale-ICH cohort, part of the Yale Longitudinal Study of Acute Brain Injury. This ongoing prospective observational study consisted of patients admitted to the Yale New Haven Hospital. Clinical data are collected through chart review and follow-up phone calls conducted by dedicated research staff at 6 months and 1 year after ICH. The median follow-up time is 1 (IQR, 0.6–1.0) year.

The same inclusion criteria were applied to identify patients in both cohorts: (1) age >18 years; (2) computed tomography (CT)-confirmed primary ICH; (3) at least 1 follow-up interview; (4) survivors of ICH after discharge. The exclusion criteria were patients without noncontrast CT (NCCT) scans or scans without complete brain coverage (Figure 1). For the dementia-related analyses, patients with dementia before ICH and patients without follow-up data were excluded. For the disability-related analysis, patients with baseline disability and patients without follow-up data on the disability status were included. In the Yale-ICH cohort, patients with baseline disability were not excluded, as this information was unavailable.

Informed consent was not sought for the present study because the Mass General Brigham and Yale IRB approved our use of anonymized patient information.

Outcome Assessment

In the MGH-ICH cohort, during each of the follow-up interviews, investigators performed cognitive assessments using the modified telephone interview for cognitive status[15,16] and assessed the functional status using the modified Rankin Scale (mRS).[17] Incident dementia after ICH was defined based on relevant *International Classification of Diseases, Ninth Revision* (*ICD-9*) codes entered in the electronic health records or modified telephone interview for cognitive status score <20.[5,15,18] The dementia status and mRS before the ICH event were obtained from either follow-up interviews or previous admissions in the electronic health records. In the Yale-ICH cohort, mRS was assessed by chart review and follow-up phone calls. In both cohorts, disability was defined as mRS score >2.

The status of dementia and disability before ICH were ascertained by searching the medical records for preexisting cognitive decline or dementia diagnoses and interviewing the patient or family members. In the analysis of post-ICH dementia, all patients with dementia before ICH or patients with missing details on pre-ICH dementia were excluded (Figure 1). In the analysis of post-ICH disability, all patients with disability (mRS score >2) before ICH or patients with missing details on baseline mRS were excluded.

CT Image Acquisition

In the MGH-ICH cohort, NCCT images were acquired from scanners from 6 different manufacturers: General Electric (GE) (82.2%), Siemens (6.6%), Philips (3.4%), Toshiba (1.7%), Mediso (0.1%), Canon (0.1%), and unknown manufacturers (5.9%). A total of 36 different scanners were found, with the most common models being: GE LightSpeed VCT (34.7%), GE LightSpeed Pro 16 (18.7%), GE LightSpeed QX/i (10.9%) and GE LightSpeed Plus (9.6%). In-plane acquisition matrix size was 512×512 for 99.7% of the scans, 1024×1024 for 0.2%, and 1280×1280 for 0.1%. The median number of axial slices was 33 (range, 18–44; IQR, 32–35).

In the Yale-ICH cohort, NCCT images were acquired from GE Discovery CT750 HD scanners. In-plane acquisition matrix size was 512×512. The number of axial slices varied between 28 and 165 slices, and the median number was 32 (IQR, 32–35).

Image Analysis

Skullstripping of the NCCT scans was performed using the histogram approach.[19] Hemorrhage was segmented from the skullstripped images using the deepbleed software.[20] Hematoma volume was obtained from the hemorrhage mask. The information regarding hemorrhage location and intraventricular extension were ascertained by the radiologists for prior investigations.[5]

NCCT was registered to the Montreal Neurological Institute (MNI) template using symmetric normalization in the ANTs package.[21] Cost-function masking was applied during registration.[22] The resulting transform was used to warp the ICH mask to the MNI space. In the MNI space, only the voxels that were covered by ICH in at least 2.5% of the subjects were retained for LSM analysis.

Frequency Map

In both the MGH-ICH and Yale-ICH cohorts, the ICH masks in the MNI space were summed and divided by their respective sample sizes to obtain the prevalence of ICH in each voxel. FreeSurfer[23] was used to generate a cortical gray matter mask, cortical white matter mask and basal ganglia mask from the MNI space. The mean prevalence of ICH in voxels in each of the masks was compared using the Wilcoxon rank-sum test.

Sparse Canonical Correlation Analysis for Neuroimaging

SCCAN used binary masks of the hemorrhage that were registered onto the MNI space. The independent variable in the SCCAN model is the presence or absence of ICH in every single voxel, that is, a binary matrix. The dependent variable is the development of

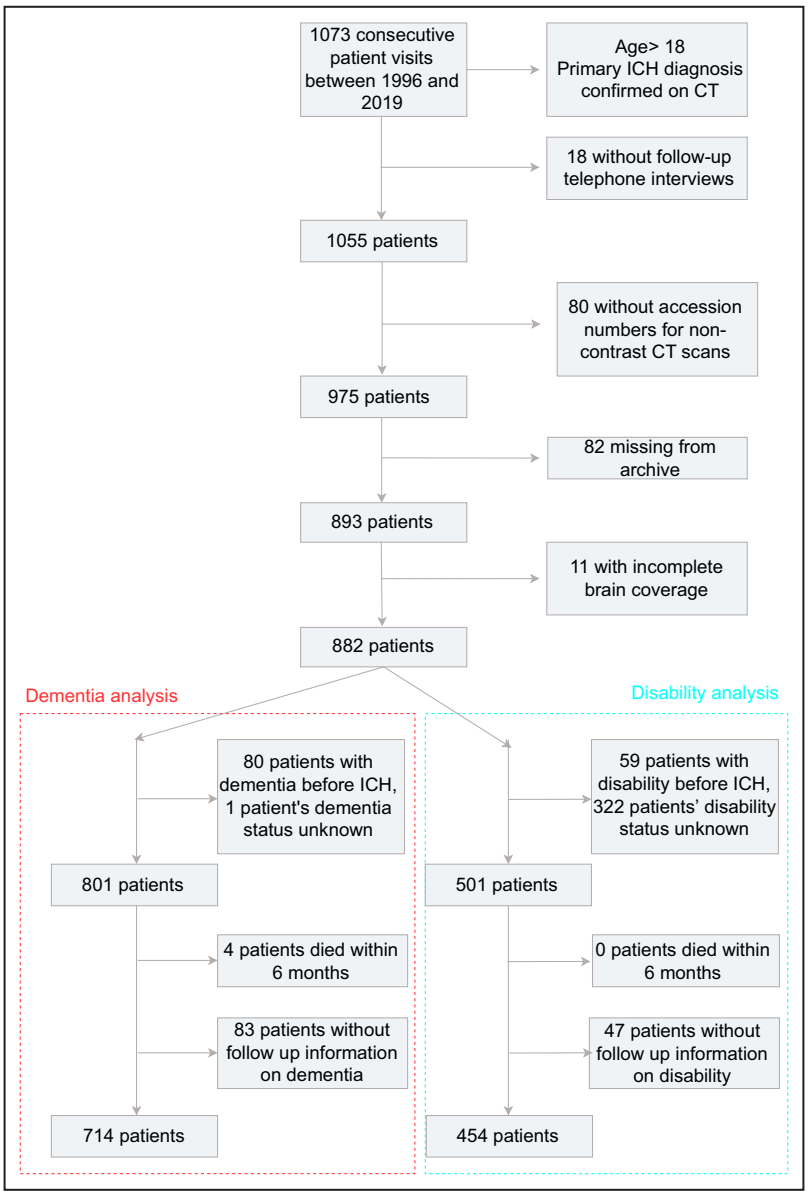

Figure 1. Patient selection flowchart in the MGH-ICH cohort.
CT indicates computed tomography; ICH, intracerebral hemorrhage; and MGH-ICH, Massachusetts General Hospital ICH Study.

dementia or disability at 6 months after ICH. SCCAN fits a multivariate model involving all the voxels with L1 regularization.[24] Patients without follow-up data at 6 months were excluded from analysis.

Voxel-Based Lesion Symptom Mapping

In each of the voxels, a multivariate Cox proportional hazard model was fitted between the presence of ICH and the time of onset of events, that is, dementia and disability. The Cox model was adjusted for age, sex and ICH volume in each voxel. Hazard ratio (HR) and the corresponding *P* value associated with the presence of a lesion in each voxel were calculated. Across all the voxels included in the analysis, the *P* values were adjusted by the Benjamini–Hochberg method.

Sensitivity Analysis

Previous studies suggested that cardiovascular risk factors, CT leukoaraiosis score, and the duration of education can influence the development of post-ICH dementia[6,25] or disability.[10] To identify potential confounding factors in the MGH-ICH data set, univariate Cox regression was performed to associate each factor with the onset of dementia or disability. The factors tested in this study were age, sex, ICH volume, history of atrial fibrillation, hypertension, diabetes,

hypercholesterolemia, previous ICH, previous cerebrovascular accident (transient ischemic attacks or stroke), history of coronary artery disease, level of education, and CT leukoaraiosis score. Education was grouped into 5 levels: 0, no education; 1, elementary school; 2, middle school; 3, high school; and 4, college or graduate level. CT leukoaraiosis score was graded according to a previous study.[26]

Variables with a *P* value of <0.05 in Cox regression were included as confounding variables. In this sensitivity analysis, a subset of the MGH-ICH cohort was identified without any missing values for any confounders. Separate subsets were created for post-ICH dementia and post-ICH disability analyses, as there were different degrees of missingness in the follow-up dementia and disability information. In each subset, voxel-wise Cox regression controlling for all the confounding factors was carried out. This analysis was not performed in the Yale-ICH cohort, due to lack of information on the CT leukoaraiosis scores and the duration of education.

Statistics and Software

The Harvard–Oxford Atlas was used to parcellate the cortical and subcortical regions while the John Hopkins University atlas was used to parcellate the white matter regions.[27] In the SCCAN analysis, for all the voxels in each region, the nonzero weights were averaged. In VLSM, for all the voxels in each region with multiple testing-adjusted *P* values <0.05, the mean and 95% CI of the HRs were obtained. The *P* values of the voxels were combined with the aggregated Cauchy association test.

For normally distributed variables as assessed with the Shapiro–Wilk test, mean±SD were reported. Otherwise, median and IQR were reported. To compare the characteristics of patients included versus excluded from a particular analysis, *P* values were obtained from unpaired *t* test for normally distributed variables, from Wilcoxon rank-sum test for nonnormally distributed variables, and from χ^2 test with Yates correction for categorical variables. All hypothesis tests were 2-sided.

All imaging processing was performed using Python version 3.8.11 on CentOS Linux 7. VLSM was implemented in Julia version 1.9 on Ubuntu 22.04. All statistical analyses were performed in R version 4.1.2 (R Foundation for Statistical Computing, Vienna, Austria) on Ubuntu 22.04.

RESULTS

Cohort Characteristics

In the MGH-ICH cohort, 1055 patients had CT-confirmed ICH and at least 1 follow-up interview call. After excluding patients without NCCT scans or scans without complete brain coverage, 882 patients were eligible for analyses (Figure 1, Table 1). For the dementia-related analyses, after excluding patients with dementia before ICH and patients without follow-up data on the dementia status, 714 patients remained with 165 having developed incident dementia. For the disability-related analysis, after excluding patients with baseline disability (mRS score >2) and patients without follow-up data on the disability status, 454 patients remained with 77 having developed disability. Patients who later developed post-ICH dementia and disability were more likely to have higher age, higher leukoaraiosis scores, higher chance of intraventricular hemorrhage, higher volume of ICH, and higher chance of lobar ICH (for post-ICH dementia but not disability; Table S1).

In the Yale-ICH cohort, among the 159 patients with CT-confirmed ICH, 13 were excluded due to missing follow-up. All of the remaining 146 patients had NCCT scans with complete brain coverage (Table S2).

Among the 882 patients in the MGH-ICH cohort, the most frequent voxels affected by ICH were in the thalamus and basal ganglia region (Figure 2). In the right hemisphere, the ICH frequency (mean prevalence, 1.36% [95% CI, 0.11–5.67]) is significantly lower than the left hemisphere (mean prevalence, 1.61% [95% CI, 0.11–6.35]; *P*<0.001). Lesion-covered voxels were more likely located in the white matter (mean prevalence, 2.05% [95% CI, 0.11–6.35]) and basal ganglia regions (4.62% [95% CI, 0.68–9.18]) than the cortical gray matter regions (1.01% [95% CI, 0.11–3.74]; *P*<0.001 for both comparisons). A similar pattern was observed in the Yale-ICH cohort (Figure S1).

Sparse Canonical Correlation for Neuroimaging (SCCAN)

In the MGH-ICH cohort (n=536), the voxels most strongly associated with dementia conversion at 6 months after ICH were located in the left temporo-occipital junction (Figure 3A). This includes the temporo-occipital parts of the left middle and inferior temporal gyri (mean weights, 0.28 [95% CI, 0.11–0.58] and 0.33 [95% CI, 0.11–0.63], respectively) and the left temporo-occipital fusiform cortex (mean weights, 0.40 [95% CI, 0.10–0.73]; Table S3). Other regions associated with dementia conversion were the left and right superior longitudinal fasciculus (mean weights, 0.26 [95% CI, 0.11–0.48] and 0.31 [95% CI, 0.11–0.59], respectively), right caudate (mean weights, 0.30 [95% CI, 0.10–0.62]) and left thalamus (mean weights, 0.29 [95% CI, 0.11–0.73]).

In the MGH-ICH cohort (n=397), regions most strongly associated with development of disability at

Table 1. Demographic of the Subsets of MGH-ICH Study Included in Each Post-ICH Outcome

	Dementia analysis (n=714)	Disability analysis (n=454)	*P*
Sex, female, n (%)	397 (55.6)	256 (56.4)	0.839
Age, y, median (IQR)	70.0 (62.0–79.0)	70.0 (61.0–80.0)	0.695*
Race, n (%)			
White	634 (88.8)	406 (89.4)	0.810
Black	40 (5.6)	25 (5.5)	1.000
Asian	19 (2.7)	13 (2.9)	0.982
Other race	10 (1.4)	7 (1.5)	1.000
Unknown race	11 (1.5)	3 (0.7)	0.284
Ethnicity, n (%)			
Hispanic	37 (5.2)	19 (4.2)	0.507
Non-Hispanic	639 (90.1)	423 (93.2)	0.091
Unknown ethnicity	33 (4.7)	12 (2.6)	0.114
Cardiovascular risk factors, n (%)			
Atrial fibrillation	122 (17.2)	75 (16.6)	0.869
Hypercholesterolemia	308 (43.7)	227 (50.8)	0.022†
Diabetes	125 (18.0)	74 (17.2)	0.788
Hypertension	545 (76.5)	348 (77.2)	0.864
Coronary artery disease	115 (16.2)	65 (14.3)	0.449
Previous cerebrovascular accident	87 (12.3)	54 (11.9)	0.938
Previous ICH	35 (4.9)	25 (5.5)	0.753
Intraventricular hemorrhage, n (%)	220 (30.8)	130 (28.6)	0.468
ICH location, n (%)			
Infratentorial ICH	78 (10.9)	51 (11.2)	0.952
Lobar ICH	327 (45.8)	204 (44.9)	0.819
Deep ICH	308 (43.2)	199 (43.8)	0.879
Left-sided ICH	302 (47.8)	183 (47.9)	1.000
ICH volume, median (IQR)	10.6 (2.9–27.3)	9.5 (2.7–25.2)	0.253*
Education (level), median (IQR)	4.0 (3.0–4.0)	4.0 (3.0–4.0)	0.159*
Leukoaraiosis score, median (IQR)	2.0 (0.0–5.0)	0.0 (0.0–5.0)	0.536*
Dementia, n (%)	165 (23.1)	77 (17.0)	0.015†
Disability, n (%)	413 (60.3)	258 (56.8)	0.271
Stroke recurrence, n (%)	95 (13.3)	57 (12.6)	0.778

P values were obtained between the characteristics in the participants included in the post-ICH dementia and disability analyses. χ^2 was applied for categorical variables and Wilcoxon rank-sum test for continuous variables. ICH indicates intracerebral hemorrhage; IQR, interquartile range; and MGH-ICH, Massachusetts General Hospital ICH Study.

**P* values derived from the Wilcoxon rank-sum test.

†Significant differences between the groups included for dementia and disability analyses.

6 months after ICH were in the right thalamus, pallidum, and posterior limb of the internal capsule (PLIC) (mean weights, 0.33 [95% CI, 0.11–0.65], 0.40 [95% CI, 0.12–0.72], and 0.53 [95% CI, 0.14–0.88], respectively; Figure 4A, Table S3). Other regions include left caudate (mean weight, 0.35 [95% CI, 0.12–0.58]), left and right superior corona radiata (mean weight, 0.33 [95% CI, 0.11–0.74] and 0.38 [95% CI, 0.12–0.71], respectively) and the right superior fronto-occipital fasciculus (mean weight, 0.41 [95% CI, 0.11–0.79]). SCCAN analysis performed on the Yale-ICH cohort (n=146) showed similar results (Figure S2), with the voxels in the right thalamus and PLIC highly associated with post-ICH disability.

Voxel-Based Lesion Symptom Mapping (VLSM)

After controlling for age, sex, and ICH volume, in the MGH-ICH cohort (n=714), the voxels most strongly associated with dementia conversion were concentrated in the left temporo-occipital junction. These include the temporo-occipital part of the left middle and inferior temporal gyri (mean HRs, 2.82 [95% CI,

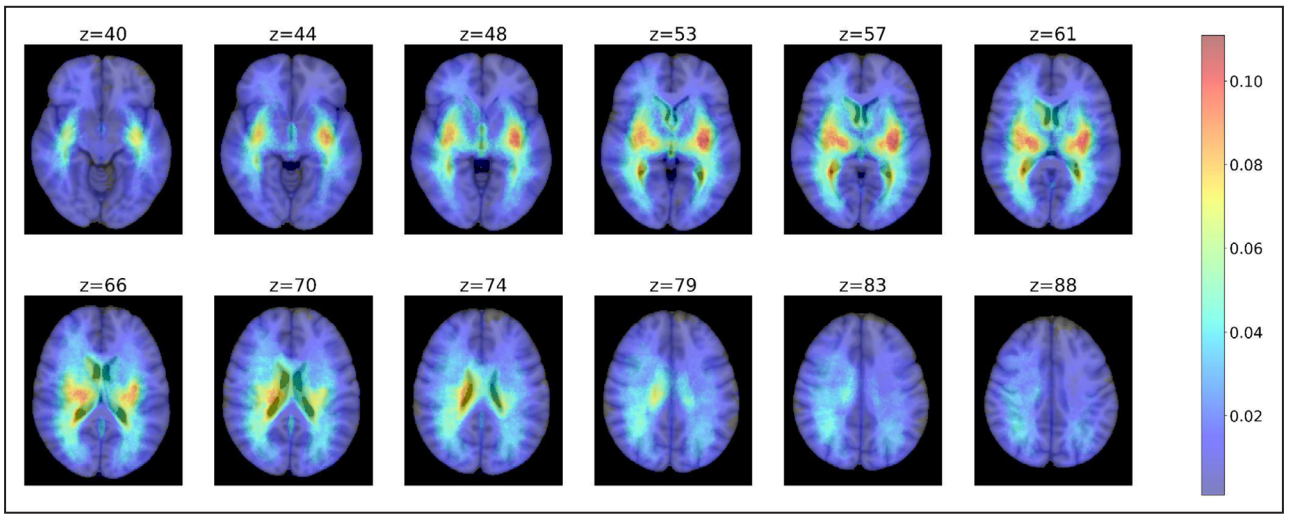

Figure 2. ICH lesion probability map.
The value in each voxel represents the proportion of ICH covering the voxel. ICH, intracerebral hemorrhage; A. Voxel weights in SCCAN, B. Voxel P-value in voxel-wise Cox regression C. Voxel hazard ratio in voxel-wise Cox regression.

2.33–3.41] and 3.62 [95% CI, 2.71–4.63], respectively), the left temporal occipital fusiform cortex (mean HR, 3.14 [95% CI, 2.20–4.37]) and the posterior division of the left superior temporal gyrus (mean HR, 2.85 [95% CI, 2.29–3.50]; Figure 3B and 3C, Table 2).

For the development of post-ICH disability, in the MGH-ICH cohort (n = 454), the most strongly related voxels were in the right PLIC, pallidum, and thalamus after adjusting for age, sex, and ICH volume (mean HRs, 2.54 [95% CI, 1.88–3.96], 2.96 [95% CI, 1.99–4.25], and 2.38 [95% CI, 1.88–3.26], respectively; Figure 4B and 4C, Table 2). The right superior longitudinal fasciculus, the right superior corona radiata, and the right cerebral peduncle were also involved (mean HRs, 2.16 [95% CI, 0.28–3.29], 2.43 [95% CI, 2.00–2.98], and 3.10 [95% CI, 2.44–3.94], respectively). Regions involved in post-ICH dementia and disability were illustrated in Figure 5. In the Yale-ICH cohort (n=146), VLSM revealed no voxels significantly associated with post-ICH disability.

Sensitivity Analysis

To adjust for variables that may confound the associations between the presence of ICH in a voxel and post-ICH outcomes, univariate Cox regression was performed between each potential confounding variable and post-ICH outcomes. In the MGH-ICH cohort, significant associations with post-ICH dementia were: age, ICH volume, level of education, CT leukoaraiosis score, presence of hypercholesterolemia, and history of coronary artery disease. Patients with missing values in these variables were excluded from subsequent analysis, yielding a sample size of 522 patients. Table S4 shows the differences in demographic features between the included and excluded patients. In this group of 522 patients, after adjusting for the 6 confounding variables, VLSM revealed a similar association of the left temporo-occipital region with dementia conversion after ICH (Figure S3).

Similarly, for post-ICH disability, the confounding variables were age, ICH volume, level of education, and presence of hypercholesterolemia. A total of 397 patients without missing values in these variables were included. Table S5 details the differences in demographic features between the included and excluded patients. After controlling for these 4 confounding variables, VLSM revealed similar associations of the right PLIC, thalamus, and pallidum with the development of disability after ICH (Figure S4).

DISCUSSION

We have conducted LSM analysis demonstrating that specific patterns of distribution of ICH lesions are linked to development of dementia and disability after ICH. We have shown that ICH in the left temporo-occipital region is associated with increased risk of dementia conversion after ICH, while ICH in the right basal ganglia and thalamus regions is associated with increased risk of developing disability. These results may provide insights into the spatial correlates of post-ICH dementia and disability and may refine ICH prognostic tools by taking account of the distribution of the ICH lesion at a voxel level.

Both SCCAN and VLSM showed that lesions in left temporo-occipital regions were associated with development of dementia. This relationship persisted after adjusting for confounders such as CT leukoaraiosis score and cardiovascular risk factors. In contrast, cognitive impairment secondary to ischemic stroke is

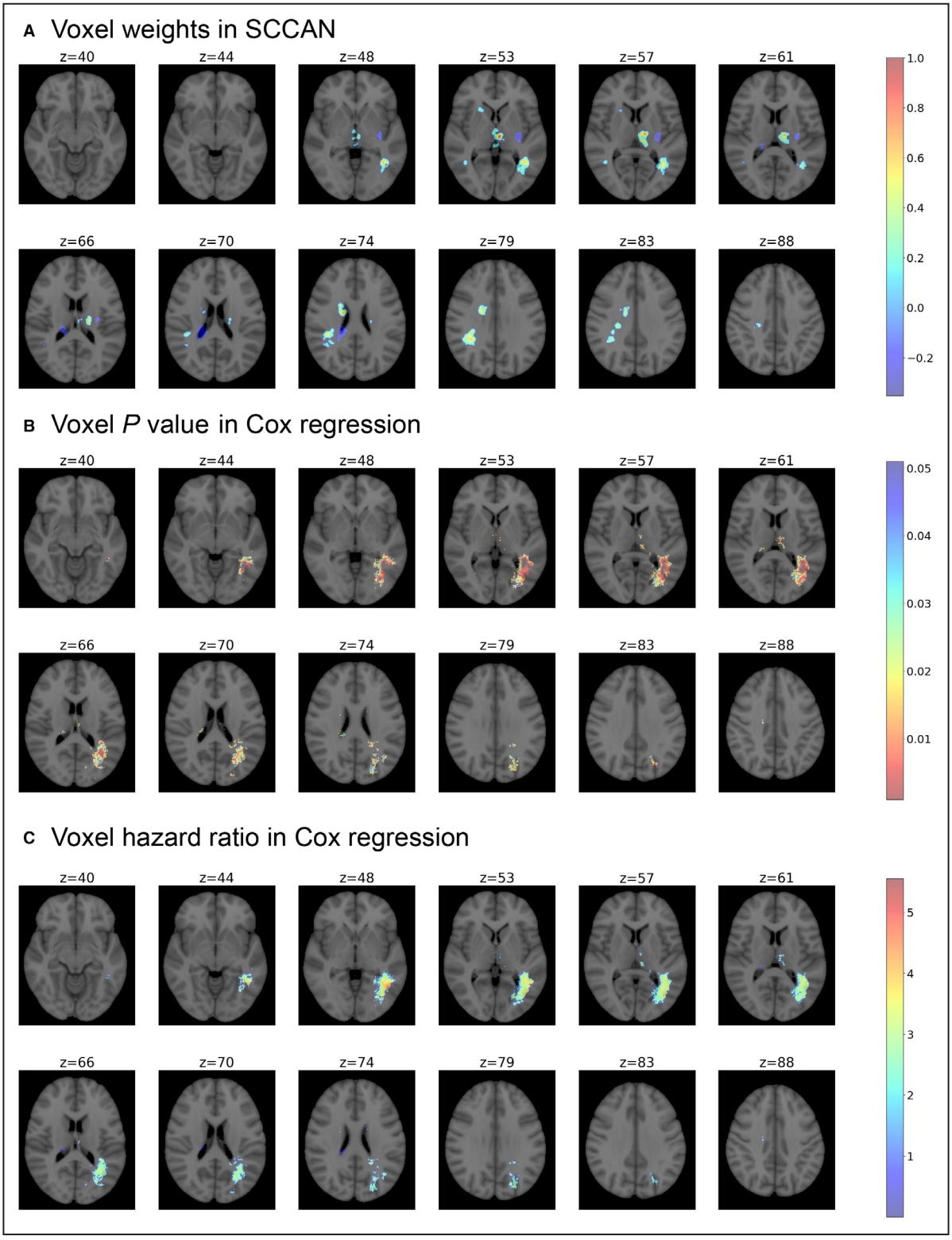

Figure 3. SCCAN (n=536) and VLSM (n=714) analyses in correlating ICH location with the onset of dementia.
SCCAN indicates sparse canonical correlation analysis for neuroimaging; and VLSM, voxel-based lesion symptom mappings.

associated with lesions in the frontotemporal regions, which is important for speech production and comprehension, and the thalamus, which has relay functions in multiple cognitive domains.[28,29] This suggests potential different mechanisms of how ischemic and hemorrhagic lesions contribute to cognitive decline. A

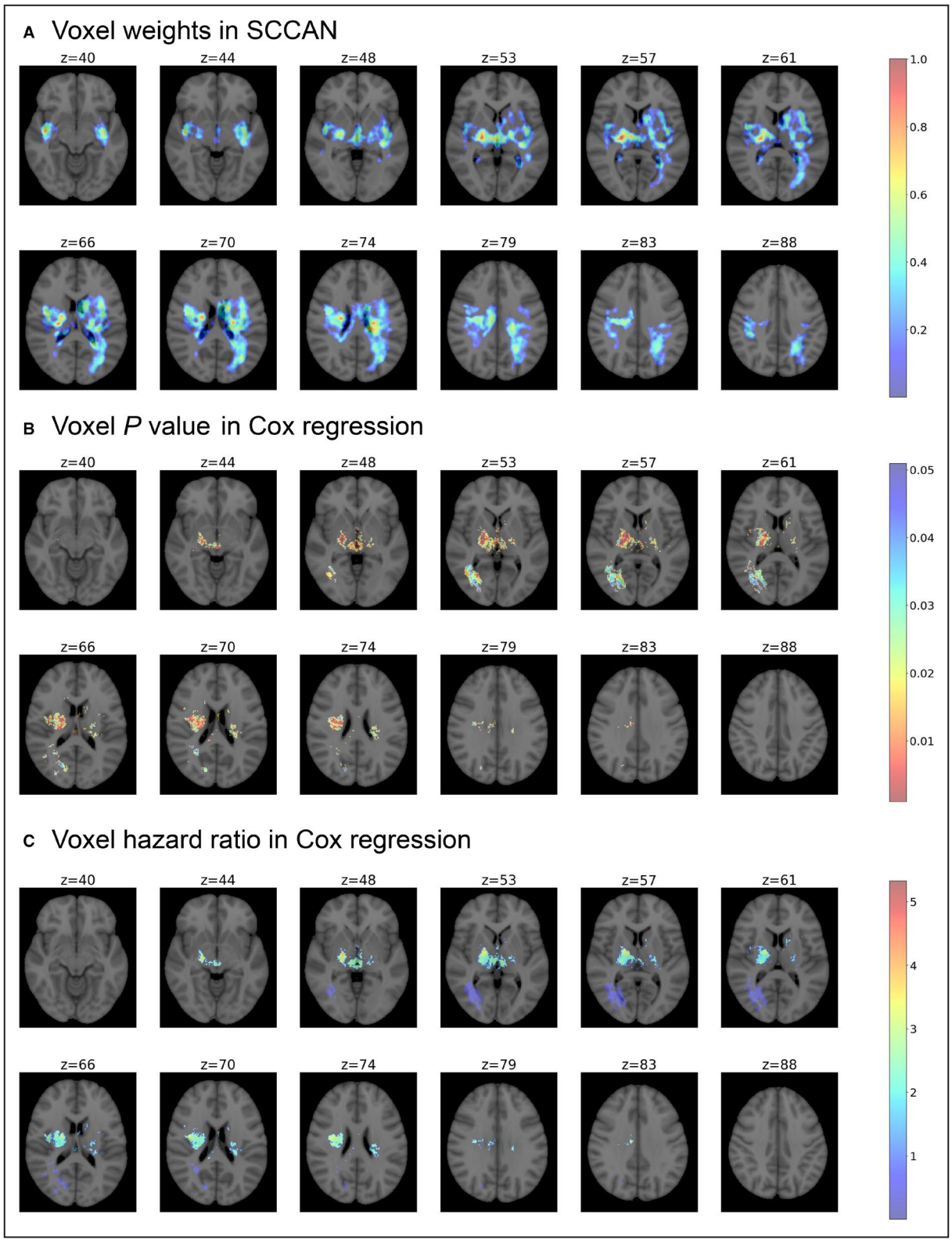

Figure 4. SCCAN (n=353) and VLSM (n=454) analyses in correlating ICH location with the onset of disability. ICH indicates intracerebral hemorrhage; SCCAN, sparse canonical correlation analysis for neuroimaging; and VLSM, voxel-based lesion symptom mappings. A. Voxel weights in SCCAN, B. Voxel P-value in voxel-wise Cox regression (i.e. VLSM), C. Voxel hazard ratio in voxel-wise Cox regression (i.e. VLSM).

Table 2. Regions With Significant Associations With Post-ICH Dementia and Disability After Controlling for Age, Sex, and ICH Volume

Region	Mean HR (95% CI)	*P*	Voxels, n	MNI coordinates		
				x	*y*	*z*
Dementia						
Left inferior temporal gyrus, temporo-occipital part	3.62 (2.71–4.63)	0.001	647	132	74	68
Left temporal occipital fusiform cortex	3.14 (2.20–4.37)	0.001	359	125	74	68
Left sagittal stratum	3.09 (2.36–4.39)	0.001	250	127	79	67
Left middle temporal gyrus, temporo-occipital part	3.23 (2.54–4.50)	0.001	1946	133	73	77
Left posterior thalamic radiation	2.78 (2.18–3.69)	0.002	3169	123	71	79
Left superior temporal gyrus, posterior division	2.85 (2.29–3.50)	0.002	205	128	82	82
Left superior longitudinal fasciculus	2.91 (2.40–3.52)	0.002	939	129	78	83
Left lateral occipital cortex, inferior division	2.98 (2.35–3.96)	0.003	2462	126	57	78
Left middle temporal gyrus, posterior division	2.82 (2.33–3.41)	0.004	234	134	83	72
Left angular gyrus	2.72 (2.37–3.22)	0.004	770	126	69	90
Disability						
Right insular cortex	1.87 (0.00–2.68)	<0.001	466	56	114	89
Right cingulate gyrus, anterior division	2.71 (1.89–4.13)	<0.001	75	83	115	101
Right lateral occipital cortex, superior division	0.31 (0.25–0.36)	<0.001	332	61	47	86
Right central opercular cortex	2.64 (2.12–3.29)	<0.001	598	52	117	91
Right pallidum	2.96 (1.99–4.25)	0.002	635	68	117	72
Right posterior limb of internal capsule	2.54 (1.88–3.96)	0.002	2882	69	112	80
Right cerebral peduncle	3.10 (2.44–3.94)	0.006	128	71	108	66
Right thalamus	2.38 (1.88–3.26)	0.006	2722	78	108	76
Right superior longitudinal fasciculus	2.16 (0.28–3.29)	0.007	484	54	107	93
Right superior corona radiata	2.43 (2.00–2.98)	0.007	1447	63	113	95

P values were aggregated across a region using the aggregated Cauchy association test. HR indicates hazard ratio; ICH, intracerebral hemorrhage; and MNI, Montreal Neurological Institute.

possible explanation is that cerebral amyloid angiopathy (CAA), which is associated with lobar ICH, contributes more to post-ICH dementia, consistent with previous works.[5,6,30] As CAA is most prevalent in the occipital region,[31,32] this could explain this temporo-occipital ICH link to post-ICH dementia.

Regarding laterality, both SCCAN and VLSM have shown that left but not right temporo-occipital ICH was associated with post-ICH dementia. The association of dementia conversion in left-sided ICH compared with right-sided ICH has been reported previously and thus corroborates our findings.[33,34] Similarly, in ischemic stroke, left-sided infarct is associated with impaired cognitive outcomes including verbal memory, language, and attention.[28,29,35] The association between left-sided lesion and poststroke dementia could relate to left-sided language centers in the majority of individuals, but will require additional investigations.[36]

Beyond these temporo-occipital associations, ICH in the superior longitudinal fasciculus bilaterally was linked to post-ICH dementia. As superior longitudinal fasciculus provides extensive connections between frontal, parietal, and temporal regions, ICH covering the superior longitudinal fasciculus may disrupt strategic connections between different cortical regions. Future studies could apply diffusion tensor imaging and tractography to understand how ICH disrupts white matter tracts.

We found that post-ICH disability, defined as a post-ICH mRS score >2, was more likely after injury in the right basal ganglia and PLIC, consistent with previous studies and again corroborating our approach.[7,10] An additional prior study showed that right basal ganglia ICH was associated with more disruption in visuospatial and executive function, whereas left basal ganglia ICH was correlated with greater impairment in speech and memory.[37] This could explain why our results favored right basal ganglia over left basal ganglia in association with post-ICH disability. Apart from basal ganglia, we found that right superior corona radiata and the right cerebral peduncle were linked to post-ICH disability, possibly because both regions, along with the PLIC, encompass the corticospinal tract,[38] which is implicated in post-ICH motor recovery.[39]

The main strength of our study is our relatively large sample size (n=714 for dementia analysis; n=454 for disability analysis) compared with previous studies employing VLSM on ICH patients, in the context of relative

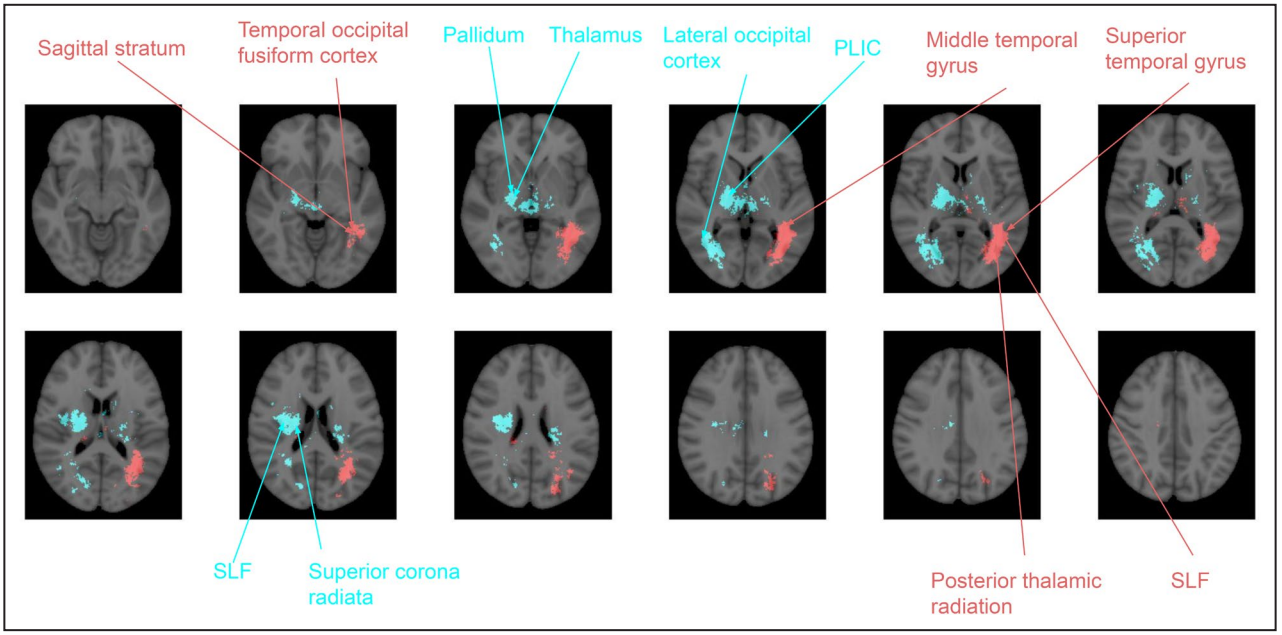

Figure 5. Illustration of the regions associated with post-ICH dementia (in red) and disability (in cyan) in VLSM analysis. ICH indicates intracerebral hemorrhage; PLIC, posterior limb of the internal capsule; and SLF, superior longitudinal fasciculus.

rarity and high early lethality of the disease.[27,40,41] The large number of scans conferred a wide range of hematoma distribution and an even coverage of the voxels in the white matter region. We additionally used an external validation cohort from a separate center to corroborate the post-ICH disability analysis. The results were robust even after adjusting for confounding vascular risk factors. We used 2 different LSM techniques: SCCAN, which confers more statistical power; and VLSM, which allows for adjustment of confounding variables and integration of longitudinal follow-up data. These 2 complementary techniques confirmed our finding that developments of post-ICH dementia and disability are associated with distinct spatial distributions of ICH.

LSM analysis allowed us to decipher the relationships between ICH location and functional outcomes at a much higher spatial resolution, compared with traditional approaches that study ICH by anatomic regions. Unlike previous studies, we did not analyze left- and right-sided ICH together or assume that left- and right-sided ICH lead to the same outcomes.[7,10] This allowed us to discover or corroborate hemispheric differences in the developments of post-ICH dementia and disability.

One limitation of our study is the limited statistical power of our MGH-ICH cohort to investigate infratentorial ICH (11% of the patients), despite being among the largest longitudinal ICH cohorts. Second, we did not investigate the differences in the spatial distribution of ICH with respect to early- and late-onset dementia. A previous study suggested that early-onset dementia is linked to ICH size and location, whereas late-onset dementia is linked to cerebral small-vessel disease and CAA.[5] Future studies should investigate whether early- and late-onset dementia are associated with different distribution patterns of ICH. Third, our analysis did not consider the mass effect from the ICH and perihematomal edema, which influence post-ICH outcomes. Fourth, while SCCAN revealed multiple clusters of voxels associated with post-ICH dementia/disability across both hemispheres, VLSM analysis tended to identify voxels in one hemisphere. The reason for the discrepancy is that VLSM has less statistical power due to the requirement of multiple testing corrections across all the voxels. Therefore, VLSM has a lower sensitivity and detects fewer regions associated with post-ICH dementia.

Fifth, either vascular risk factors or education status information were missing in 27% and 13% of the participants in sensitivity analyses related to post-ICH dementia and disability respectively (Table S6). This has limited our statistical power to detect true associations in the sensitivity analysis. Furthermore, in the sensitivity analysis, stroke severity was not adjusted due to the lack of information in the National Institutes of Health Stroke Scale in the MGH-ICH cohort. However, as ICH location is a determinant of stroke severity and stroke severity does not determine ICH location, we do not expect adjusting for stroke severity would affect the VLSM results.

Furthermore, both VLSM and SCCAN identified associations, rather than cause–effect relationships between ICH locations and post-ICH dementia/disability. For example, our finding that occipital lobe ICH is associated

with dementia does not necessarily mean that disruption of occipital lobe function in ICH causes dementia. This relationship could be confounded by variables not adjusted by our sensitivity analyses such as CAA status.

Finally, neuropsychiatric assessment during the first 6 months of ICH could be confounded by consequences of post-ICH delirium[41] and aphasia, which were not assessed in this study. This could potentially lead to false positives in dementia diagnosis and false positives in the voxels correlating with dementia.

In conclusion, our LSM analysis revealed the spatial correlates of ICH distribution with post-ICH dementia and disability, which could aid understanding of the cortical and subcortical structures implicated in the clinical trajectory after ICH, and may assist in development of prognostic models.

ARTICLE INFORMATION

Received August 1, 2024; accepted October 10, 2024.

Affiliations

Center for Genomic Medicine, Massachusetts General Hospital, Boston, MA (Y.C., S.A.M., J.R., E.M., C.D.A.); Broad Institute of Harvard and MIT, Cambridge, MA (Y.C., S.A.M., J.R., E.M., C.D.A.); Henry and Allison McCance Center for Brain Health, Massachusetts General Hospital, Boston, MA (Y.C., S.A.M., J.R., E.M., C.D.A.); Department of Neurology, Yale School of Medicine, New Haven, CT (C.A.R., V.T.L., S.P., K.S., G.J.F.); Yale Center for Brain and Mind Health, New Haven, CT (C.A.R., V.T.L., S.P., K.S., G.J.F.); Department of Neurology and Neurophysiology, University Medical Center Freiburg, Faculty of Medicine, University of Freiburg, Germany (A.H.); and Department of Neurology, Brigham and Women's Hospital, Boston, MA (C.D.A.).

Acknowledgments

Y. Chen conceived the study. Dr Mayerhofer and S. Mora collected the data from the MGH-ICH cohort. Drs Rivier and Payabvash and V. Torres Lopez collected the data for the Yale-ICH cohort. Y. Chen and Dr Rivier performed all the statistical analyses. Y. Chen and Dr Rivier drafted the initial version of the manuscript. All authors read and revised the manuscript.

Sources of Funding

C.D.A. is supported by National Institutes of Health R01NS103924, U01NS069673, American Heart Association 18SFRN34250007, American Heart Association–Bugher 21SFRN812095, and the MGH McCance Center for Brain Health. J.R. receives research grants from National Institutes of Health and the American Heart Association–Bugher Foundation. A.H. is supported by the Berta-Ottenstein-Program for Advanced Clinician Scientists, Faculty of Medicine, University of Freiburg, Germany.

Disclosures

Dr Rosand reports compensation from the National Football League for consulting and expert witness services and from Eli Lilly for consultant services, all unrelated to this work. Dr Anderson has received sponsored research support from Bayer AG and has consulted for ApoPharma unrelated to this work. Dr Mayerhofer is now a full-time employee of Regeneron Pharmaceuticals. The remaining authors have no disclosures to report.

Supplemental Material

Tables S1–S6
Figures S1–S4

REFERENCES

1. Xiong L, Reijmer YD, Charidimou A, Cordonnier C, Viswanathan A. Intracerebral hemorrhage and cognitive impairment. *Biochim Biophys Acta (BBA)—Mol Basis Dis*. 2016;1862:939–944. doi: 10.1016/j.bbadis.2015.12.011
2. Rost NS, Smith EE, Chang Y, Snider RW, Chanderraj R, Schwab K, FitzMaurice E, Wendell L, Goldstein JN, Greenberg SM, et al. Prediction of functional outcome in patients with primary intracerebral hemorrhage. *Stroke*. 2008;39:2304–2309. doi: 10.1161/STROKEAHA.107.512202
3. Kazim SF, Ogulnick JV, Robinson MB, Eliyas JK, Spangler BQ, Hough TJ, Martinez E, Karimov Z, Vidrine DW, Schmidt MH, et al. Cognitive impairment after intracerebral hemorrhage: a systematic review and meta-analysis. *World Neurosurg*. 2021;148:141–162. doi: 10.1016/j.wneu.2021.01.026
4. van Asch CJ, Luitse MJ, Rinkel GJ, van der Tweel I, Algra A, Klijn CJ. Incidence, case fatality, and functional outcome of intracerebral haemorrhage over time, according to age, sex, and ethnic origin: a systematic review and meta-analysis. *Lancet Neurol*. 2010;9:167–176. doi: 10.1016/S1474-4422(09)70340-0
5. Biffi A, Bailey D, Anderson CD, Ayres AM, Gurol EM, Greenberg SM, Rosand J, Viswanathan A. Risk factors associated with early vs delayed dementia after intracerebral hemorrhage. *JAMA Neurol*. 2016;73:969–976. doi: 10.1001/jamaneurol.2016.0955
6. Moulin S, Labreuche J, Bombois S, Rossi C, Boulouis G, Hénon H, Duhamel A, Leys D, Cordonnier C. Dementia risk after spontaneous intracerebral haemorrhage: a prospective cohort study. *Lancet Neurol*. 2016;15:820–829. doi: 10.1016/S1474-4422(16)00130-7
7. Eslami V, Tahsili-Fahadan P, Rivera-Lara L, Gandhi D, Ali H, Parry-Jones A, Nelson LS, Thompson RE, Nekoobakht-Tak S, Dlugash R, et al. Influence of intracerebral hemorrhage location on outcomes in patients with severe intraventricular hemorrhage. *Stroke*. 2019;50:1688–1695. doi: 10.1161/STROKEAHA.118.024187
8. Juvela S. Risk factors for impaired outcome after spontaneous intracerebral hemorrhage. *Arch Neurol*. 1995;52:1193–1200. doi: 10.1001/archneur.1995.00540360071018
9. Arboix A, Comes E, García-Eroles L, Massons J, Oliveres M, Balcells M, Targa C. Site of bleeding and early outcome in primary intracerebral hemorrhage. *Acta Neurol Scand*. 2002;105:282–288. doi: 10.1034/j.1600-0404.2002.1o170.x
10. Delcourt C, Sato S, Zhang S, Sandset EC, Zheng D, Chen X, Hackett ML, Arima H, Hata J, Heeley E, et al. Intracerebral hemorrhage location and outcome among INTERACT2 participants. *Neurology*. 2017;88:1408–1414. doi: 10.1212/WNL.0000000000003771
11. Wittstock M, Meyer K, Klinke J, Grossmann A, Walter U, Storch A. Effects of insular involvement on functional outcome after intracerebral hemorrhage. *Acta Neurol Scand*. 2021;144:559–565. doi: 10.1111/ane.13496
12. Englander RN, Netsky MG, Adelman LS. Location of human pyramidal tract in the internal capsule: anatomic evidence. *Neurology*. 1975;25:823–826. doi: 10.1212/WNL.25.9.823
13. Inoue K, Madhyastha T, Rudrauf D, Mehta S, Grabowski T. What affects detectability of lesion–deficit relationships in lesion studies? *NeuroImage: Clin*. 2014;6:388–397. doi: 10.1016/j.nicl.2014.10.002
14. Pustina D, Avants B, Faseyitan OK, Medaglia JD, Coslett HB. Improved accuracy of lesion to symptom mapping with multivariate sparse canonical correlations. *Neuropsychologia*. 2018;115:154–166. doi: 10.1016/j.neuropsychologia.2017.08.027
15. Barber M, Stott DJ. Validity of the telephone interview for cognitive status (TICS) in post-stroke subjects. *Int J Geriatr Psychiatry*. 2004;19:75–79. doi: 10.1002/gps.1041
16. de Jager CA, Budge MM, Clarke R. Utility of TICS-M for the assessment of cognitive function in older adults. *Int J Geriatr Psychiatry*. 2003;18:318–324. doi: 10.1002/gps.830
17. van Swieten JC, Koudstaal PJ, Visser MC, Schouten HJ, van Gijn J. Interobserver agreement for the assessment of handicap in stroke patients. *Stroke*. 1988;19:604–607. doi: 10.1161/01.STR.19.5.604
18. Pendlebury ST, Welch SJV, Cuthbertson FC, Mariz J, Mehta Z, Rothwell PM. Telephone assessment of cognition after transient ischemic attack and stroke: modified telephone interview of cognitive status and telephone Montreal cognitive assessment versus face-to-face Montreal cognitive assessment and neuropsychological battery. *Stroke*. 2013;44:227–229. doi: 10.1161/STROKEAHA.112.673384
19. Balan AGR, Traina AJM, Ribeiro MX, Marques PMA, Traina C Jr. Smart histogram analysis applied to the skull-stripping problem in T1-weighted MRI. *Comput Biol Med*. 2012;42:509–522. doi: 10.1016/j.compbiomed.2012.01.004
20. Sharrock MF, Mould WA, Ali H, Hildreth M, Awad IA, Hanley DF, Muschelli J. 3D deep neural network segmentation of intracerebral hemorrhage:

development and validation for clinical trials. *Neuroinformatics*. 2021;19:403–415. doi: 10.1007/s12021-020-09493-5
21. Avants BB, Tustison N, Johnson H. Advanced Normalization Tools (ANTS). 2014.
22. Andersen SM, Rapcsak SZ, Beeson PM. Cost function masking during normalization of brains with focal lesions: still a necessity? *NeuroImage*. 2010;53:78–84. doi: 10.1016/j.neuroimage.2010.06.003
23. Billot B, Greve DN, Puonti O, Thielscher A, Van Leemput K, Fischl B, Dalca AV, Iglesias JE. SynthSeg: segmentation of brain MRI scans of any contrast and resolution without retraining. *Med Image Anal*. 2023;86:102789. doi: 10.1016/j.media.2023.102789
24. Avants BB, Libon DJ, Rascovsky K, Boller A, McMillan CT, Massimo L, Coslett HB, Chatterjee A, Gross RG, Grossman M. Sparse canonical correlation analysis relates network-level atrophy to multivariate cognitive measures in a neurodegenerative population. *NeuroImage*. 2014;84:698–711. doi: 10.1016/j.neuroimage.2013.09.048
25. Biffi A, Murphy MP, Kubiszewski P, Kourkoulis C, Schwab K, Gurol ME, Greenberg SM, Viswanathan A, Anderson CD, Rosand J. APOE genotype, hypertension severity and outcomes after intracerebral haemorrhage. *Brain Commun*. 2019;1:fcz018. doi: 10.1093/braincomms/fcz018
26. Uniken Venema SM, Marini S, Lena UK, Morotti A, Jessel M, Moomaw CJ, Kourkoulis C, Testai FD, Kittner SJ, Brouwers HB, et al. Impact of cerebral small vessel disease on functional recovery after intracerebral hemorrhage. *Stroke*. 2019;50:2722–2728. doi: 10.1161/STROKEAHA.119.025061
27. Hess F, Foerch C, Keil F, Seiler A, Lapa S. Association of lesion pattern and dysphagia in acute intracerebral hemorrhage. *Stroke*. 2021;52:2921–2929. doi: 10.1161/STROKEAHA.120.032615
28. Weaver NA, Kuijf HJ, Aben HP, Abrigo J, Bae H-J, Barbay M, Best JG, Bordet R, Chappell FM, Chen CPLH, et al. Strategic infarct locations for post-stroke cognitive impairment: a pooled analysis of individual patient data from 12 acute ischaemic stroke cohorts. *Lancet Neurol*. 2021;20:448–459. doi: 10.1016/S1474-4422(21)00060-0
29. Munsch F, Sagnier S, Asselineau J, Bigourdan A, Guttmann CR, Debruxelles S, Poli M, Renou P, Perez P, Dousset V, et al. Stroke location is an independent predictor of cognitive outcome. *Stroke*. 2016;47:66–73. doi: 10.1161/STROKEAHA.115.011242
30. Boyle PA, Yu L, Nag S, Leurgans S, Wilson RS, Bennett DA, Schneider JA. Cerebral amyloid angiopathy and cognitive outcomes in community-based older persons. *Neurology*. 2015;85:1930–1936. doi: 10.1212/WNL.0000000000002175
31. Attems J, Jellinger KA, Lintner F. Alzheimer's disease pathology influences severity and topographical distribution of cerebral amyloid angiopathy. *Acta Neuropathol*. 2005;110:222–231. doi: 10.1007/s00401-005-1064-y
32. Kövari E, Herrmann FR, Hof PR, Bouras C. The relationship between cerebral amyloid angiopathy and cortical microinfarcts in brain ageing and Alzheimer's disease. *Neuropathol Appl Neurobiol*. 2013;39:498–509. doi: 10.1111/nan.12003
33. Garcia PY, Roussel M, Bugnicourt JM, Lamy C, Canaple S, Peltier J, Loas G, Deramond H, Godefroy O. Cognitive impairment and dementia after intracerebral hemorrhage: a cross-sectional study of a hospital-based series. *J Stroke Cerebrovasc Dis*. 2013;22:80–86. doi: 10.1016/j.jstrokecerebrovasdis.2011.06.013
34. Gong L, Gu Y, Yu Q, Wang H, Zhu X, Dong Q, Xu R, Zhao Y, Liu X. Prognostic factors for cognitive recovery beyond early Poststroke cognitive impairment (PSCI): a prospective cohort study of spontaneous intracerebral hemorrhage. *Front Neurol*. 2020;11:278. doi: 10.3389/fneur.2020.00278
35. Ankolekar S, Renton C, Sare G, Ellender S, Sprigg N, Wardlaw JM, Bath PMW; ENOS Trial Investigators. Relationship between poststroke cognition, baseline factors, and functional outcome: data from "efficacy of nitric oxide in stroke" trial. *J Stroke Cerebrovasc Dis*. 2014;23:1821–1829. doi: 10.1016/j.jstrokecerebrovasdis.2014.04.022
36. Puppala GK, Gorthi SP, Chandran V, Gandeti R, Rao SS. Prevalence of cognitive impairment and dementia after intracerebral hemorrhage. *Ann Indian Acad Neurol*. 2023;26:952–957. doi: 10.4103/aian.aian_731_23
37. Su C-Y, Chen H-M, Kwan A-L, Lin Y-H, Guo N-W. Neuropsychological impairment after hemorrhagic stroke in basal ganglia. *Arch Clin Neuropsychol*. 2007;22:465–474. doi: 10.1016/j.acn.2007.01.025
38. Ackley WB, Adolphe TS, Aeddula NR, Adagi S, Agasthi P, Ahmad S, Ahmed A, Ahmed F, Ahmed I, Ahmed R, Emos MC, Khan Suheb MZ, Agarwal S. Neuroanatomy, internal capsule. *StatPearls*. StatPearls Publishing; 2024. http://www.ncbi.nlm.nih.gov/books/NBK542181/
39. Li J, Wei XH, Liu YK, Chen LS, Zhu ZQ, Hou SY, Fang XK, Wang ZQ. Evidence of motor injury due to damaged corticospinal tract following acute hemorrhage in the basal ganglia region. *Sci Rep*. 2020;10:16346. doi: 10.1038/s41598-020-73305-8
40. Lee J-Y, King C, Stradling D, Warren M, Nguyen D, Lee J, Riola MA, Montoya R, Patel D, Le VH, et al. Influence of hematoma location on acute mortality after intracerebral hemorrhage. *J Neuroimaging*. 2014;24:131–136. doi: 10.1111/j.1552-6569.2012.00766.x
41. Marrama F, Kyheng M, Pasi M, Pierre Rutgers M, Moulin S, Diomedi M, Leys D, Cordonnier C, Hénon H, Casolla B. Early-onset delirium after spontaneous intracerebral hemorrhage. *Int J Stroke*. 2022;17:1030–1038. doi: 10.1177/17474930211059636